Journal of the Iranian Chemical Society
https://doi.org/10.1007/s13738-017-1282-y

ORIGINAL PAPER

KIT-6-anchored sulfonic acid groups as a heterogeneous solid acid catalyst for the synthesis of aryl tetrazoles

Alireza Najafi Chermahini[1] · **Nikzad Andisheh**[1] · **Abbas Teimouri**[2]

Received: 21 May 2017 / Accepted: 23 December 2017

Abstract

In the current study, a simple, environmentally benign and cost-effective method is presented for the preparation of 5-substituted-1*H*-aryltetrazoles. To this goal, mesoporous KIT-6 silica anchored with sulfonic acid (–SO_3H) groups via post-grafting modification was synthesized using the sol–gel method and characterized by XRD, TGA, FTIR, BET, TEM and SEM techniques. For the preparation of tetrazole derivatives, the effect of various parameters such as catalyst amount, aryl nitrile:azide ratio, temperature and reaction time was tested. The hybrid organic/inorganic catalyst could be recovered easily through a simple filtration and reused multiple times without significant loss in activity.

Keywords Post-grafting modification · Sol–gel method · Sulfonated KIT-6 · 5-Substituted-1*H*-tetrazoles

Introduction

Tetrazoles are known as a family of synthetic organic heterocycles, which have been of much attention due to their numerous applications [1]. A series of tetrazole compounds with high energy content have been examined as new explosives with high-performance ability as replace for TNT and formulation of solid rocket propellants [2, 3]. In addition, they are bioisosteres of the carboxylic acid group in drug design [4] and play important roles in coordination chemistry as dentate aromatic *N*-donor ligands [5]. Also, they have been utilized in photography [6], synthons [7], various biological activities [8], dye-sensitized solar cells [9–11] and information recording systems [12]. Generally, preparation of these heterocycles is the cycloaddition reaction of azide salts and aryl or alkyl nitriles [13]. The choice of a proper catalyst is critical in achieving good results. In the earlier synthetic methods, homogeneous catalysts such as BF_3-OEt_2 [14], $AlCl_3$ [15], $AgNO_3$ [16], $Fe(OAc)_2$ [17], TBAF [18], copper triflates [19] and zinc(II) salts [20] were used. Since for homogeneous catalysts, the difficulty in separation of the products from the catalyst is a major problem, the heterogeneous alternatives have been received considerable attention. So far, various heterogeneous catalysts have been reported by research groups such as nanocrystalline ZnO [21], Cu_2O [22], Zn/Al hydrotalcite [23], COY zeolite [24], modified MCM-41 [25], mesoporous ZnS nanospheres [26], montmorillonite [27], modified montmorillonite clays [28] and sulfated zirconia [29].

Mesoporous KIT-6 [30] material with high thermal stability and surface area, large and tunable pore diameter and narrow particle size distributions has been interested for numerous applications such as sensors, drug delivery, catalysis, adsorption, lithium-ion batteries and nanodevices [31–40]. This mesoporous material that is similar to MCM-48 but benefits from much larger diameter [41] shows a three-dimensional cubic *Ia3d* symmetry with the interpenetrating bicontinuous network of chiral channels [42]. These features let it to permit diffusion of reactant to its channels and active sites easier than other mesoporous materials [43]. However, it should be noted that due to its electronically neutral character, the pristine KIT-6 material has a few weak Brönsted and Lewis acid sites. The acidity character could be improved by incorporation of sulfonic acid groups into the framework by employing post-grafting methods (Scheme 1). Here we have introduced a catalytic method for the synthesis of 5-substituted-1*H*-tetrazoles using $PrSO_3H$–KIT-6 material.

✉ Alireza Najafi Chermahini
anajafi@cc.iut.ac.ir; najafy@gmail.com

[1] Department of Chemistry, Isfahan University of Technology, Isfahan 84156-83111, Iran

[2] Chemistry Department, Payame Noor University, Tehran 19395-3697, Iran

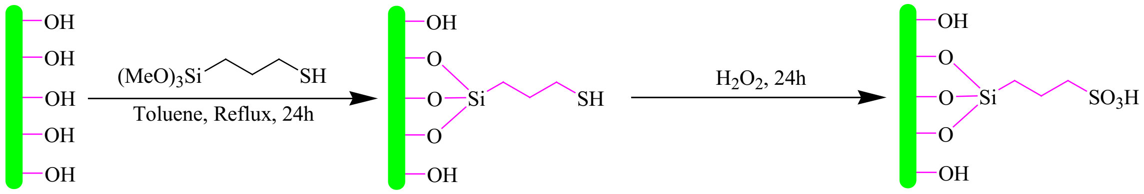

Scheme 1 Schematic representation of the preparation of KIT-6-$PrSO_3H$

Experimental

Materials

Pluronic P123 triblock co-polymer with molecular weight of 5800 (EO20PO70EO20), (3-mercaptopropyl)trimethoxysilane (MPTMS) and sodium azide were purchased from Aldrich Chemical Inc. Tetraethyl orthosilicate (TEOS) and hydrogen peroxide (H_2O_2) (30%, w/v solution) were gotten from Dae-Jung, S. Korea. Aryl nitriles were purchased from Merck. Double-distilled water was used to prepare all aqueous solutions.

Characterization techniques

Thermogravimetric analysis (TGA) of the sulfonated KIT-6 was conducted by using a STA503 TA instrument (Hullhorst, Germany) analyzer under nitrogen atmosphere in the temperature range of 25–800 °C, with a heating rate of 10 °C/min. Low-angle X-ray diffraction (XRD) patterns of samples were collected on a Bruker D8 advance X-ray diffractometer operating at 40 kV and 40 mA by using a CoKα radiation. The morphology of the pristine KIT-6 and functionalized one was determined by administering SEM analysis on a Philips XI30 microscope, and TEM was carried out by a Philips CN120 device. N_2 adsorption–desorption isotherms were measured using a Quantachrome Auto sorb IQ MP device. Quantification of the $PrSO_3H$ groups loaded on KIT-6 was carried out on a Leco CHNS model 932 elemental analyzer. The content of grafted sulfonic acid groups was calculated with NaOH solution (0.01 M). The full adsorption–desorption isotherm was obtained using Brunauer–Emmett–Teller (BET) method at various relative pressures. The FTIR spectra were recorded on a JASCO FT/IR-680 PLUS spectrometer using KBr pellets. NMR spectra were recorded on a Bruker 400 Ultrashield NMR, using DMSO-d6 as the solvent.

Preparation of mesoporous silica KIT-6

The synthesis of pristine silica KIT-6 was done by employing Pluronic P123 as template and 1-butanol as co-solvent and diluted hydrochloric acid. Similar to a previously reported procedure [44], the molar of the starting reaction mixture was set to 0.017 P123:1 TEOS:1.31 BuOH: 1.83 HCl: 195 H_2O. For this purpose, 7.0 g of Pluronic P123 was dissolved in 250 mL of water containing 14 mL of HCl solution (6 N). Afterward, 1-butanol (4.0 g) was added to the solution, under vigorous stirring at 35 °C for 1.5 h. Then, TEOS (15.0 g) was added to the homogeneous clear solution, and stirring was allowed to be continued for 24 h at the same temperature. Finally, the white solid precipitate was filtered and dried at 100 °C for 12 h, followed by calcination at 550 °C to remove templates for 6 h.

Functionalization of KIT-6

For functionalization of mesoporous KIT-6 material with sulfonic acid groups, to a solution of 5 mL (3-mercaptopropyl)trimethoxysilane (MPTMS) dissolved in 30 mL dried toluene, was added 2 g of KIT-6 and the mixture was refluxed for 24 h. Afterward, the hybrid organic/inorganic solid was filtered and transferred to a Soxhlet extractor to bring out unreacted MPTMS molecules from the pores in the methanol. Then, the solid materials were dried at 90 °C for 12 h. The thiol groups then were oxidized to sulfonic acid by hydrogen peroxide. For this purpose under vigorous, to 2 g of mercaptopropylated KIT-6 suspended in water was added 30 mL of H_2O_2 (35%) at room temperature for 12 h. Finally, the KIT-6 material grafted with sulfonic acid groups was filtered, washed with acetone and water, and dried at 90 °C in oven.

General procedure for the synthesis of aryl tetrazoles

In a round-bottom flask, 0.2 g benzonitrile (2 mmol) and 0.4 g sodium azide (6 mmol), were added to 10 mL DMF. To this mixture, 20 mg of functionalized KIT-6 was added and the reaction mixture was refluxed. The progress of reaction was monitored by TLC (75:25 ethyl acetate/*n*-hexane). After completion of the reaction, the reaction mixture was cooled and filtered. The solid materials were washed three times with acetone and then with the water. The catalyst was collected and dried to activation for next run. The product was obtained by acidification of solution with hydrochloric acid (5 mL, 6 M). The precipitate was filtered and recrystallized from a water/ethanol mixture to get pure product as a white powder, yield: 88%.

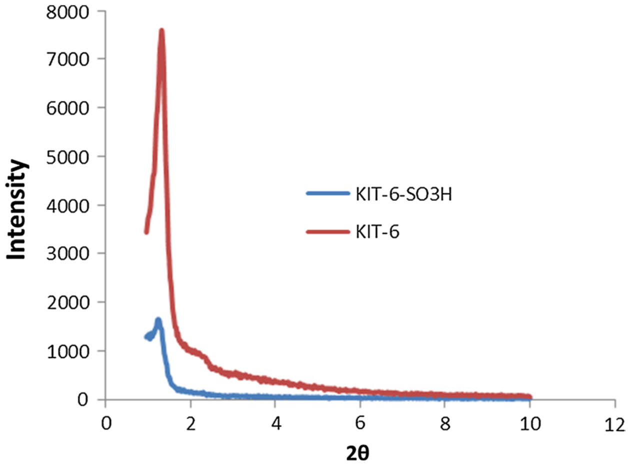

Fig. 1 Small-angle XRD patterns of KIT-6 after calcination and KIT-6–Pr–SO_3H solid acid catalyst

Results and discussion

Catalyst characterization

XRD studies

The mesoporosity of ordered KIT-6 solids was determined by XRD analysis. The powder XRD patterns of the KIT-6 after calcination and $PrSO_3H$-KIT-6 are shown in Fig. 1. A sharp signal near 2θ of 1.3° and one weak peak near 2.1° are corresponding to the (100) and (220) planes of the ordered KIT-6 material after calcination, respectively [42]. The XRD pattern of KIT-6 after incorporation of alkyl groups is presented in Fig. 1. As it can be seen, after modification of surface with propyl sulfonic acid groups, intensity of signals decreased, indicating that scattering contrast between channels and walls decreased.

Nitrogen physisorption

Nitrogen adsorption/desorption isotherms of pure KIT-6 and KIT-6- $PrSO_3H$ are brought in Fig. 2. In addition, the BET surface area, pore volume and pore size distribution (PSD) of samples are presented in Table 1. The isotherms are of type IV with a sharp capillary condensation in the range of P/P_0 0.4–0.7. In addition, the hysteresis for both

Table 1 Characteristics of catalysts

Sample	$S_{BET}(m^2/g)^a$	$V_{Total}(cm^3/g)$	PSD (nm)
KIT-6	762	0.74	4.31
KIT-6-$PrSO_3H$	307	0.25	3.15

[a] Determined by N_2 adsorption using the Brunauer–Emmett–Teller method

Fig. 2 Nitrogen sorption data of pristine KIT-6 (left) and KIT-6-$PrSO_3H$ (right)

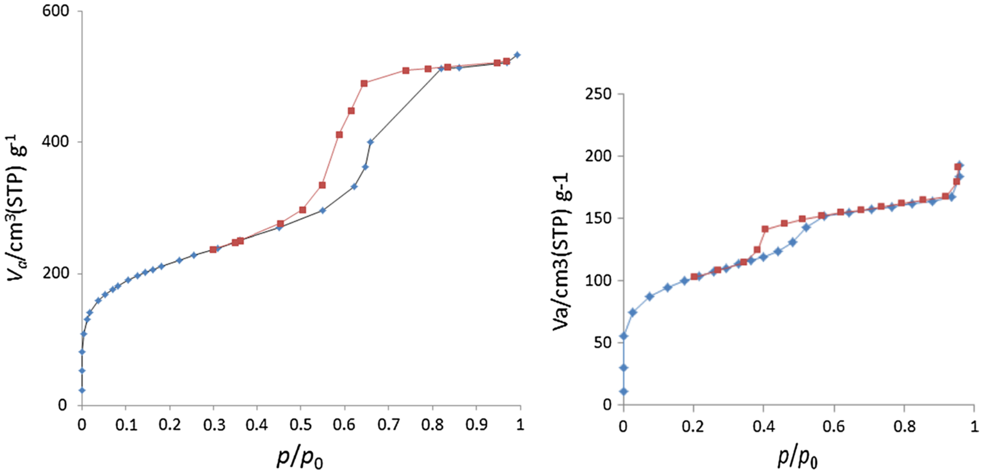

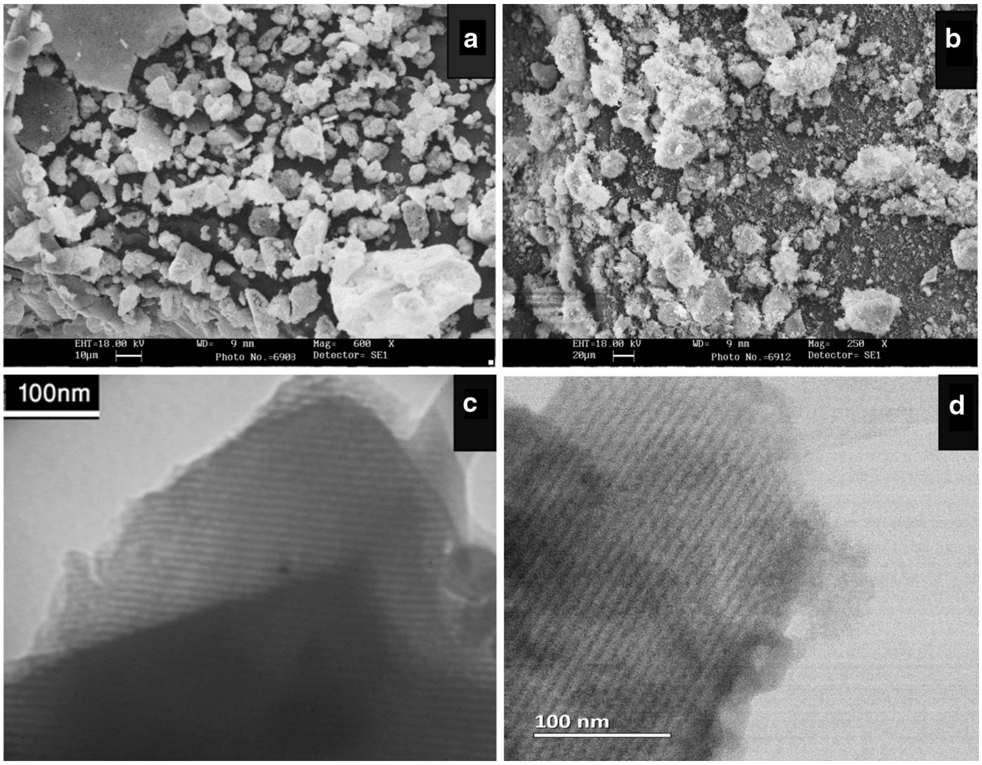

Fig. 3 SEM images of KIT-6 (**a**) and KIT-6–Pr–SO_3H (**b**) TEM images of KIT-6 (**c**) and KIT-6–Pr–SO_3H (**d**)

samples shows H1 loop indicating the uniformity of the synthesized KIT material and modified catalyst [45, 46].

The pore sizes were calculated from the pore size distribution of the adsorption branch of the nitrogen isotherm using BJH method. The results indicated decrease in PDS after mercaptopropylation of KIT-6 material which attributed to occupation of mesopores. In addition, the BET surface area after functionalization of KIT-6 decreased from 762 to 307 m^2/g.

SEM and TEM characterization

Figure 3a and b shows the surface morphology of the pristine KIT-6 and KIT-6-PrSO_3H solid acid catalyst observed through scanning electron micrograph. The SEM photograph demonstrates a non-uniform structure containing both small and rough particles, which reported previously for KIT-6 [47, 48]. Also, the SEM image indicated that the particles were not perturbed after incorporation of Pr–SO_3H groups. Figure 3 (c, d) shows transmission electron microscopy images of KIT-6 (c) and modified KIT-6 (d). The images show highly mesoporous structures with honey-comb morphology and open-ended lamellar type of pores.

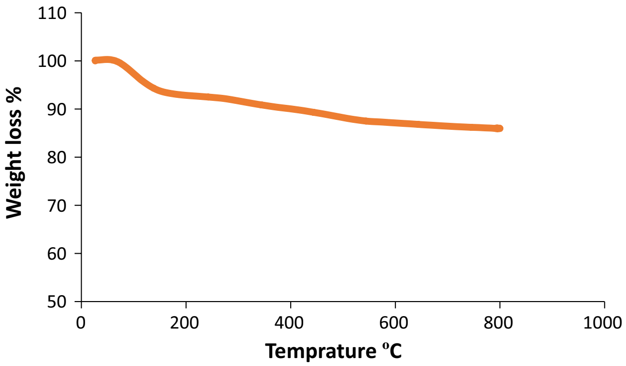

Fig. 4 TGA curve for KIT-6–Pr–SO_3H catalyst

Thermogravimetric analysis (TGA)

To estimate the amount of organic material supported on inorganic mesoporous compound, the thermogravimetric analysis was employed. The TGA results for KIT-SO_3H catalyst are presented in Fig. 4. A closer look at the picture indicates the catalyst showed two distinct weight losses: (I) a lower mass reduction occurred in the range of 50–140 °C due to water removal, and (II) elimination of propyl sulfonic acid groups in the range between 200 and 800 °C.

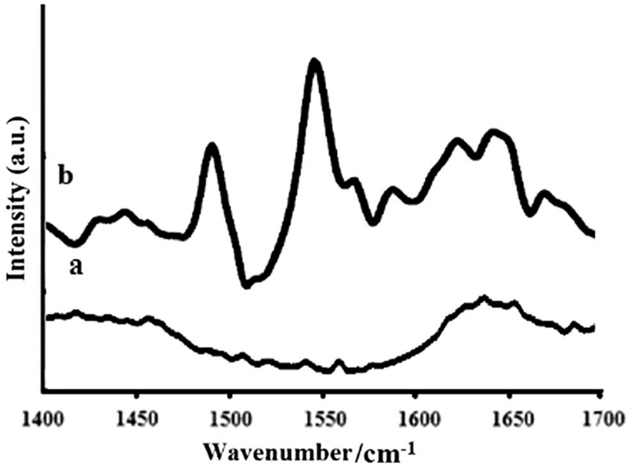

Fig. 5 FTIR spectra of KIT-6-PrSO$_3$H (**a**) and KIT-6-PrSO$_3$H after pyridine adsorption (**b**)

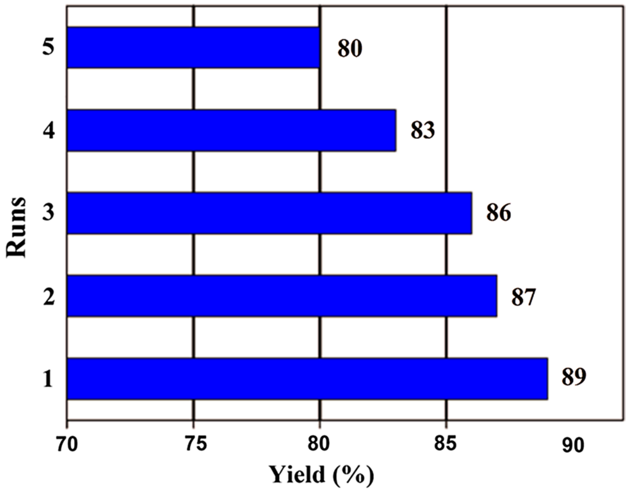

Fig. 6 Reaction yields for five runs in the presence of the recycled catalyst

Based on this observation, total organic content of catalyst was estimated to be about % 5.

FTIR

The FTIR spectroscopy was used for the evaluation of acidic character of the catalyst after adsorption of pyridine as the probe molecule in the 1400–1700 cm^{-1} region [49]. Figure 5 shows the spectra of KIT-6-PrSO$_3$H before and after pyridine adsorption. A closer look at Fig. 6 indicates four bands at 1487, 1548, 1594 and 1643 cm^{-1} were appeared after pyridine deposition. The sample exhibited band at 1594 cm^{-1} due to hydrogen-bonded pyridine and a band at 1487 cm^{-1}, which can be assigned to pyridine associated with both Bronsted and Lewis sites.

In addition, pyridinium ion ring vibration due to pyridine bound to Bronsted acid sites was observed at 1548 cm^{-1} and a band appeared at 1643 cm^{-1} that assigned to the Lewis acid sites. In order to evaluate the acid capacity number of KIT-6-PrSO$_3$H catalyst, acid–base titration method was done. Based on the titration, the acid capacity was found to be 1.03 meq (H$^+$)/g SiO$_2$, which is in consistent with TGA data.

Catalytic studies

After preparation and characterization of KIT-6-PrSO$_3$H catalyst, catalytic activity of compound in the preparation of aryl tetrazoles from aryl nitriles was explored. To optimize reaction conditions, we tested the reaction of benzonitrile (**1a**) as a model compound with sodium azide to obtain 5-phenyl-1*H*-tetrazole (**1b**). Our study started with the evaluation of effect of the catalyst amount in the model reaction (Scheme 2).

Different amounts (5, 10, 20 and 30 mg) of KIT-6-PrSO$_3$H catalyst were examined. The experiments on the effect of catalyst loading showed that 20 mg of the KIT-6-SO$_3$H is adequate to conversion of 2 mmol benzonitrile to corresponding aryl tetrazole (Table 2, entries 1–4). It became apparent that low loading of catalyst needs longer reaction times and decreasing the reaction yield. In the second step, the effect of sodium azide:benzonitrile ratio was investigated. The results showed that an excess amount of NaN$_3$ was critical. The results indicated that benzonitrile: sodium azide molar ratios 1:1, 1:3 and 1:5 gave 42, 84 and 89% product yield after 34, 22 and 16 h, respectively (Table 2, entries 3, 5, and 6). Therefore, the 1:3 benzonitrile: sodium azide ratio was selected for next runs.

With keeping in hands the mentioned conditions, the reaction was performed in different temperatures. The low temperature at the same catalyst loading did not give better yields (Table 2 entries 7, 8). The optimum reaction conditions were 120 °C and 16 h. Subsequently, the effect of the different solvents on the reaction was examined (Table 3). Low polar solvents such as toluene, chloroform and THF could not be suitable for this reaction even after prolonged heating under the optimized conditions. Also, with H$_2$O and NMP, yields were comparatively poor (Table 3, entries 1–5). However, alcohols were better and they could be more

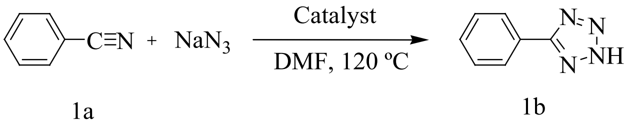

Scheme 2 Reaction of benzonitrile and sodium azide to form 5-phenyl-1*H*-tetrazole catalyzed by KIT-6–Pr–SO$_3$H

Table 2 Optimization of different proportions of KIT-6–Pr–SO_3H nanocatalyst and the effect of catalyst and sodium azide amount and temperature on the formation of 1-substituted 1H-tetrazoles[a]

Entry	Solvent	Catalyst loading (mg)	NaN_3 (mmol)	Temp. (°C)	Time (h)	Yield[b] (%)
1	DMF	5	3	120	30	65
2	DMF	10	3	120	26	72
3	DMF	20	3	120	16	89
4	DMF	30	3	120	16	86
5	DMF	20	1	120	34	42
6	DMF	20	5	120	22	84
7	DMF	20	3	100	26	74
8	DMF	20	3	110	24	75
9	DMF	20	3	140	20	90
10	DMF	20	3	Reflux	18	92

[a] Reaction condition: benzonitrile (1 mmol, 103 mg) and solvent (10 ml)

[b] Isolated yield

Table 3 Effect of different solvents on the reaction times[a]

Entry	Solvent	Catalyst (mg)	Temp. (°C)	Yield[b] (%)
1	Toluene	20	120	Trace
2	Chloroform	20	120	Trace
3	THF	20	120	Trace
4	H_2O	20	120	31
5	NMP	20	120	44
6	MeOH	20	120	62
7	EtOH	20	120	55
8	DMSO	20	120	85
9	DMF	20	120	89

[a] Reaction condition: benzonitrile (1 mmol, 103 mg), sodium azide (3 mmol, 0.2 gr) and solvent (10 ml)

[b] Isolated yield of product

efficiently achieved (Table 3, entries 6 and 7). The experimental results showed that DMF and DMSO were good solvents, but due to its easier workup DMF was chosen as the most suitable solvent (Table 3, entries 8 and 9).

This process is found to be significantly useful for synthesis of various aryl tetrazoles (Table 4, entries 1–11). Under the optimum conditions, reaction of sodium azide and some aryl nitriles gave the corresponding tetrazoles in good yields.

The results presented in Table 4 indicated that the nature of substituent had no significant influence on the reactivity of the nitrile; also, aromatic rings with electron donor groups, as well as cycles with electron-withdrawing ones showed similar yields. It is noteworthy that the reported yields in Table 4 are after recrystallization. Since the solubility of aryl tetrazoles with functional groups such as COOH and COH which can form hydrogen bonding may be increased in water, the isolated yields were slightly decreased.

It is known that one of the most important features of a catalyst is its ability for the regeneration and reusing. With regard to this, the stability and resumption of KIT-6-SO_3H catalyst were examined in the model reaction of benzonitrile and sodium azide under the optimized reaction conditions. After separation of the catalyst from the reaction mixture by simple filtration, the catalyst was washed with water and acetone and dried at 80 °C in oven overnight. The activity of the catalyst in five consecutive runs suggested that the catalyst is active and can be used several times (Fig. 6).

To show the advantages of KIT-6–Pr–SO_3H catalyst over some reported catalysts, the activity of this material in the reaction of benzonitrile with sodium azide was compared with well-known existing methods (see Table 5).

As listed in Table 5, our procedure gave high yield in lesser reaction times. In addition, some of these methods use hazardous materials as catalyst and involve tedious purification of products.

Conclusion

To conclude, in this study we addressed the synthesis of KIT-6 material functionalized with propyl sulfonic acid moiety as a hybrid inorganic/organic catalyst. The catalyst was systematically characterized and BET, TGA, SEM, and TEM, together with XRD studies, all confirmed the successful attachment of sulfonic acid groups to the walls of KIT-6. The catalyst was then successfully applied in the conversion of aromatic nitriles to the corresponding tetrazoles derivatives. The results showed that application of a benzonitrile:sodium azide 1:3 ratio and 20 mg of KIT-6–Pr–SO_3H catalyst in DMF is the best reaction condition for the synthesis of aryl tetrazoles. Various solvents were examined, and it was found that when polar and aprotic solvents such as DMF were used, the best results were observed. The KIT-6–Pr–SO_3H catalyst was regenerated, and

Table 4 Preparation of 5-substituted-1*H*-tetrazoles in the presence of KIT-6–Pr–SO_3H catalyst [a]

Entry	Substrate	Product	Yield[a] (%)	Mp °C
1	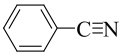	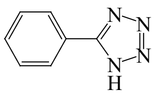	89	215–217
2	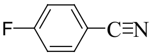	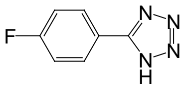	88	113–115
3	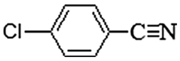	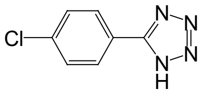	80	263–265
4	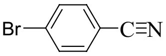	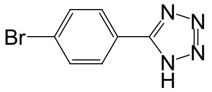	79	268–270
5	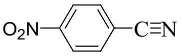	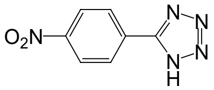	77	217–219
6	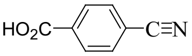	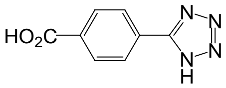	71	249–251
7	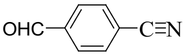	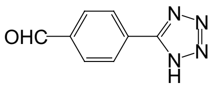	73	183–185
8	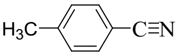	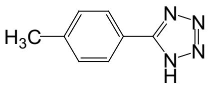	75	252–254
9	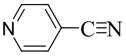	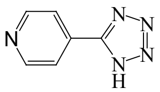	75	236–238
10	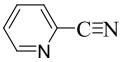	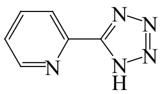	78	210–212
11	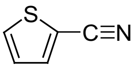	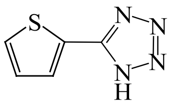	83	201–203

Conditions: benzonitrile (1 mmol, 103 mg), sodium azide (3 mmol, 0.2 gr) and solvent (10 ml)

[a] Isolated yield of product

Table 5 Comparison of various catalysts in the synthesis of 5-substituted 1H-Tetrazoles[a]

Entry	Catalyst	Temp. (°C)	Yield (%)	Time (h)	Reference
1	Sulfated zirconia	110–120	90	24	[28]
2	$Fe(OAc)_2$	80	56	24	[16]
3	Graphene	120	63	36	[50]
4	Silica sulfuric acid	Reflux	88	5	[51]
5	$BaWO_4$	120	75	24	[52]
6	$ZnBr_2$	Reflux	76	24	[2]
7	Mesoporous ZnS	120	86	36	[53]
8	Nano-ZnO	120	72	14	[20]
9	$FeCl_3$-SiO_2	120	79	12	[54]
10	KIT-6–Pr–SO_3H	120	89	16	This work

the results of five consecutive runs showed that the catalyst could be recovered and reused several times.

Acknowledgements The authors wish to acknowledge the financial supports from the Isfahan University of Technology (Iran) for the research work carried out.

References

1. R.N. Butler, A.R. Katritzky, C.W. Rees, E.F.V. Scriven, *Comprehensive Heterocyclic Chemistry*, vol. 4 (Pergamon, Oxford, 1996)
2. Z.P. Demko, K.B. Sharpless, J. Org. Chem. **66**, 7945–7950 (2001)
3. H.X. Gao, J.M. Shreeve, Chem. Rev. **111**, 7377–7436 (2001)
4. G.F. Holland, J.N. Pereira, J. Med. Chem. **10**, 149–154 (1967)
5. R.J. Hert, Bioorg. Med. Chem. **10**, 3379–3393 (2002)
6. L.M.T. Frija, A. Ismael, M.L.S. Cristiano, Molecules **15**, 3757–3774 (2010)
7. A. Burger, Prog. Drug Res. **37**, 287–371 (1991)
8. A. Patil, S. Ganguly, S. Surana, J. Chem. Sci. **122**, 443–450 (2010)
9. Z.J. Chermahini, A.N. Chermahini, H.A. Dabbagh, B. Rezaei, N. Irannezhad, Spectrochimica Acta A **178**, 79–85 (2017)
10. Z.J. Chermahini, A.N. Chermahini, H.A. Dabbagh, A. Teimouri, J. Energy Chem. **24**, 770–778 (2015)
11. Z.J. Chermahini, A.N. Chermahini, H.A. Dabbagh, B. Rezaei, N. Irannezhad, J. Iran. Chem. Soc. **14**, 1549–1556 (2017)
12. G.I. Koldobskii, V.A. Ostrovskii, Usp. Khim. **63**, 847–865 (1994)
13. T. Jin, S. Kamijo, Y. Yamamoto, Tetrahedron Lett. **45**, 9435–9437 (2004)
14. A. Kumar, R. Narayanan, H. Shechter, J. Org. Chem. **61**, 4462–4465 (1996)
15. D.P. Matthews, J.E. Green, A.J. Shuker, J. Comb. Chem. **2**, 19–23 (2000)
16. P. Mani, A.K. Singh, S.K. Awasthi, Tetrahedron Lett. **55**, 1879–1882 (2014)
17. J. Bonnamour, C. Bolm, Chem. Eur. J. **15**, 4543–4545 (2009)
18. D. Amantini, R. Beleggia, F. Fringuelli, F. Pizzo, L. Vaccaro, J. Org. Chem. **69**, 2896–2898 (2004)
19. L. Bosch, J. Vilarrasa, Angew. Chem. Int. Ed. **46**, 3926–3930 (2007)
20. F. Himo, P.Z. Demko, L. Noodleman, K.B. Sharpless, J. Am. Chem. Soc. **124**, 12210–12216 (2002)
21. M.L. Kantam, K.B. Shiva Kumar, C. Sridhar, Adv. Synth. Catal. **347**, 1212–1214 (2005)
22. T. Jin, F. Kitahara, S. Kamijo, Y. Yamamoto, Tetrahedron Lett. **49**, 2824–2827 (2008)
23. M. Lakashmi, K.B. Kantam, Shiva Kumar, Kp Raja, J. Mol. Catal. A **247**, 186–188 (2006)
24. V. Rama, K. Kanagaraj, K. Pitchumani, J. Org. Chem. **76**, 9090–9095 (2011)
25. A.N. Chermahini, MKh Omran, H.A. Dabbagh, Gh Mohammadnezhad, A. Teimouri, New J. Chem. **39**, 4814–4820 (2015)
26. M.L. Kantam, V. Balasubrahmanyam, K.B. Shiva, Kumar. Synth. Commun. **36**, 1809–1814 (2006)
27. A.N. Chermahini, A. Teimouri, F. Momenbeik, A. Zarei, Z. Dalirnasab, A. Ghaedi, M. Roosta, J. Heterocyclic Chem. **47**, 913–922 (2010)
28. A.N. Chermahini, A. Teimouri, A. Moaddeli, Heteroat. Chem. **2**, 168–173 (2011)
29. A. Teimouri, A.N. Chermahini, Polyhedron **30**, 2606–2610 (2011)
30. F. Kleitz, S.H. Choi, R. Ryoo, Chem. Commun. **17**, 2136–2137 (2003)
31. U. Ciesla, F. Schüth, Microporous Mesoporous Mater. **27**, 131–141 (1999)
32. M.E. Davis, Nature **417**, 813–821 (2002)
33. F. Schüth, W. Schmidt, Adv. Mater. **14**, 629–638 (2002)
34. F. Schüth, Angew. Chem. Int. Ed. **42**, 3604–3622 (2003)
35. M. Hartmann, Chem. Mater. **17**, 4577–4593 (2005)
36. A. Taguchi, F. Schüth, Microporous Mesoporous Mater. **77**, 1 (2005)
37. M. Vallet-Regi, F. Balas, D. Arcos, Angew. Chem. Int. Ed. **46**, 7548 (2007)
38. C.D. Liang, Z.J. Li, S. Dai, Angew. Chem. Int. Ed. **47**, 3696 (2008)
39. Y.F. Shi, Y. Wan, D.Y. Zhao, Chem. Soc. Rev. **40**, 3854 (2011)
40. H. Tüysüz, F. Schüth, Adv. Catal. **55**, 127 (2012)
41. T.W. Kim, F. Kleitz, B. Paul, R. Ryoo, J. Am. Chem. Soc. **127**, 7601–7610 (2005)
42. H. Oveisi, C. Anand, A. Mano, S.S. Al-Deyab, P. Kalita, A. Beitollahi, A. Vinu, J. Mater. Chem. **20**, 10120–10129 (2010)
43. H. Hafizi, A.N. Chermahini, M. Saraji, G. Mohammadnezhad, Chem. Eng. J. **294**, 380–388 (2016)
44. Z. Luan, M. Hartmann, D. Zhao, W. Zhou, L. Kevan, Chem. Mater. **11**, 1621–1627 (1999)
45. F. Kleitz, F. Berube, R. Guillet-Nicolas, C. Yang, M. Thommes, J. Phys. Chem. C **114**, 9344–9355 (2010)
46. J. Sun, Q. Kan, Z. Li, G. Yu, H. Liu, X. Yang, Q. Huo, J. Guan RSC Adv **4**, 2310–2317 (2014)
47. A. Boulaoued, I. Fechete, B. Donnio, M. Bernard, P. Turek, F. Garin, Microporous Mesoporous Mater. **155**, 131–142 (2012)
48. A. Prabhu, L. Kumaresan, M. Palanichamy, V. Murugesan, Appl. Catal. A. **360**, 59–65 (2009)
49. E.P. Parry, J. Catal. **2**, 371–379 (1963)
50. G. Qi, W. Zhang, Y. Dai, Res. Chem. Intermed. **41**, 1149–1155 (2015)
51. Z. Du, C. Si, Y. Li, Y. Wang, G. Lu, Int. J. Mol. Sci. **13**, 4696–4703 (2012)
52. J. He, B. Li, F. Chen, Z. Xu, G. Yin, J. Mol. Catal. A **304**, 135–138 (2009)
53. L. Lang, H. Zhou, M. Xue, X. Wang, Z. Xu, Mater. Lett. **106**, 443–446 (2013)
54. M. Nasrollahzadeh, Y. Bayat, D. Habibi, S. Moshaee, Tetrahedron Lett. **50**, 4435–4438 (2009)